

Analyzing 4-C marine seismic data from the Valhall field, Norway

Carlos Rodriguez-Suarez, Robert R. Stewart, Xinxiang Li and John C. Bancroft

ABSTRACT

A 2-D seismic line using four-component (4-C) receivers - a 3-C geophone and hydrophone - laid on the sea bottom was acquired in 1996 by PGS. The survey was undertaken by Amoco and its partners over the Valhall Field, offshore Norway. The main objective of the survey was to provide a better image of a chalk reservoir. Converted (P-S) waves are used, as P-P waves are strongly attenuated and scattered due to the presence of gas in the layers over the reservoir.

The vertical component of the geophone and hydrophone showed a largely reflection-free zone for the target at the middle of the section. Four processing flows were applied to the radial receiver component: conventional CDP processing (for possible P-S-S events, i.e., a conversion at the sea bottom), common conversion point (CCP) asymptotic binning, P-S DMO, and equivalent offset migration (EOM). We did not find convincing evidence of a P-S-S event. The final result for the radial component processed for P-S events was good, as a continuous image for the target was obtained. A very good overall section was generated using the asymptotic binning method. The EOM method gave better results than converted-wave DMO at practically the same CPU time. The transverse component has reflections for the same events mapped by the radial component, but with much lower continuity.

To investigate the presence of P-wave energy on the radial and transverse components, the processing flow for the P-P wave was applied to the radial and transverse data. In addition, the asymptotic binning P-S flow was applied to the vertical channel data. The results show that: 1) little P-S energy is present on the vertical component, and 2) only small P-P energy occurs in radial and transverse components.

Severe periodic notches in the amplitude spectra, probably due to reverberation in the water layer, were observed in all components. An algorithm is being developed to attenuate the reverberation in the geophone (mainly for the radial component, where the signal bandwidth is strongly affected) using the hydrophone measurements.

VALHALL FIELD: GEOLOGY AND SEISMIC ASPECTS

The Valhall field, operated by Amoco Norway Oil Company and partners, is located in the southernmost part of the Norwegian North Sea (Figure 1a). The water depth in the area is about 70 m.

The main reservoir (70% of oil in place) is a chalk (Tor Formation, Maastrichtian Age). One model for the reservoir genesis is that sub-aqueous movements (debris flows, slumps, slides and turbidities) created fast accumulations of redeposited chinks, generating anomalies in the chalk thickness (Leonard and Munns, 1987; D'Angelo *et al.*, 1997). Farmer and Barkved (1997) present a new model, using 3-D seismic data and biostratigraphy, where syn-depositional faulting and reworking play an important role in reservoir thickness variation. They conclude that graben areas created during continuous uplift on Late Cretaceous and Early Tertiary were protected from erosion and became depositional centers for the reworked chalk.

The reservoir facies has porosity in excess of 40% over most of the field, permeability between 2 to 15 mD, and abrupt thickness variation (0 to 80 m). These high primary porosity values are due to high rates of deposition and lack of consolidation and cementation. They were preserved due to extreme overpressure in the reservoir caused by hydrocarbon migration, in a complex interplay of depositional modes with oil migration timing, burial history, diagenesis and insoluble residue concentrations (Leonard and Munns, 1987; D'Angelo *et al.*, 1997; Farmer and Barkved, 1997).

As with most oil fields producing from chalk reservoirs in offshore Norway, the trap is structural/stratigraphic. The reservoir depth is around 2400 m. The highest uncertainty in the exploration is the presence of porosity, as the reservoir facies is surrounded by pelagic facies. There is a strong variation in reservoir quality, with the thickest areas presenting best porosities and permeabilities (Leonard and Munns, 1987; D'Angelo *et al.*, 1997; Farmer and Barkved, 1997).

The quality of conventional seismic data is poor because the overburden layers (Tertiary marine shales) are highly gas charged. This causes scattering and signal attenuation of pure P-wave energy. Some other techniques, as VSP, flattened seismic sections and seismic inversion have been used to help with this problem (Munns and Mullen, 1987).

The main purpose of the seismic analysis is to differentiate the reservoir and non-reservoir chalk facies. D'Angelo *et al.* (1997) report an integrated study combining geological models (sedimentology of chalk deposition, burial histories and reworking of autochthonous chalk), petrophysical information from core samples (which showed association between increasing porosity and decreasing velocities for P- and S-waves), and surface seismic analysis (stratigraphic processing, velocity analysis with a 125 m interval, modeling, inversion and AVO) that allowed the detection and mapping of high-porosity reservoir-quality chinks. They found anomalously low velocity zones, including a gas chimney, at the high and down flank regions of the field. The conclusions of their work were confirmed by an oil discovery.

Landro *et al.* (1995), assuming a horizontally layered model and neglecting anisotropy effects, performed an AVO inversion in conventional data over the Valhall field. They considered a single layer over the reservoir, and used P- and S-wave velocities and densities from empirical relationships and well log data. Shear velocities were determined mainly from variation of reflection amplitude with angle of incidence. Corrections for absorption were made using a quality factor (Q) of 250.

The V_p/V_s ratios obtained from their work vary between 1.12 and 1.56. According to the authors, these low values do not agree with ultrasonic core measurements, although predicted porosity values from their study were confirmed by a discovery well.

The potential reserves of the Valhall and adjacent Hod fields (Figure 1b) area has been recently estimated to be more than 1 billion barrels of oil (Farmer and Barkved, 1997). A map in depth of the top of the chalk, from Leonard and Munns (1987), is presented in Figure 1b.

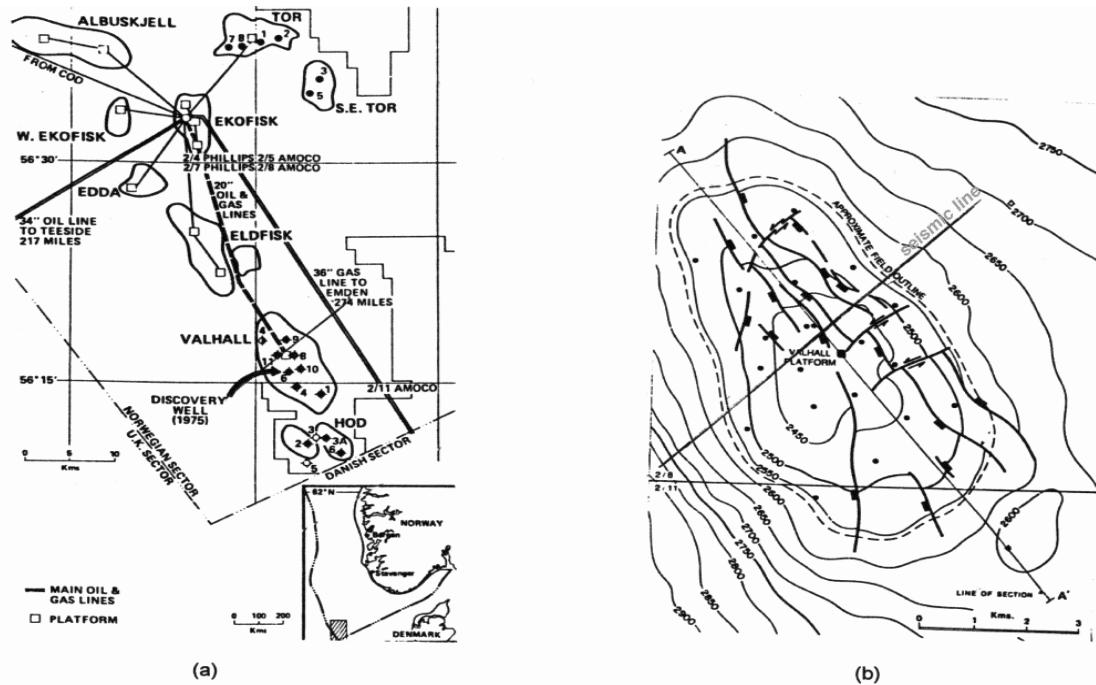


Fig. 1. (a) Localization of Valhall field; (b) indication of seismic line on a depth map of the top of the chalk (from Leonard and Munns, 1987).

SEISMIC ACQUISITION

PGS Reservoir Services AS acquired the sea-bottom seismic survey in June 1996, using a shooting boat (“Professor Polshkov”) and a receiver (“Bergen Surveyor”) vessel. The unique aspect of the acquisition is the receiver system. A cable with eight receiver units – each unit weighting 50 kg and containing one gimballed multicomponent (3-C) geophone and one hydrophone – was laid on the sea bottom (Berteussen *et al.*, 1997; Kommedal *et al.*, 1997). Each unit location defines a station position.

The cable, with an anchor on one end, is laid on the sea bottom. The receiver vessel pulls the cable to straighten it. The final cable position is obtained from two acoustic transducers on the cable. After the receiver system is ready, the source vessel

traverses directly overhead and parallel to it. Offsets to about 8 km on each side of the center of the cable are used. At the end of the shooting line, the receiver cable was moved 200 m in line for the next position in the southwest direction. The same shooting pattern was repeated. In the total, 40 lines were shot, giving approximately 200,000 traces/component in total (Berteussen *et al.*, 1997, Kommedal *et al.*, 1997). During the shooting, the receiver vessel was positioned 500 m ahead and 150 m off-line. This acquisition system is named by PGS as “Dragged Array” (Berteussen *et al.*, 1997).

The receiver and shot point distance is 25 m. The cable and shooting directions are approximately along the azimuth 237° (Figure 1b). The maximum nominal fold, at the center of the line, is around 300. The approximate position for CDPs range is shown in Figure 1b. The sample rate is 2 ms and record time 11.5 s.

As the sea bottom is composed of hard sand, good coupling is believed to have resulted (Kommedal *et al.*, 1997). No information is available about measurements on the geophone orientation. The position for each receiver was probably obtained through interpolation between the cable’s extremes, although this could not be confirmed.

PROCESSING SEQUENCE ON PROMAX: RESULTS AND COMMENTS

The first step is to resample (with an anti-alias filter) the data from 2 ms to 4 ms to facilitate analysis of this large dataset. If any signal is present over 125 Hz, it probably occurs only in the very shallow part of the section. After preliminary processing, an offset limit of 4.0 km (except for equivalent offset migration and converted-wave DMO in the radial channel, where 3.5 km was used) and a maximum time limitation of 6.0 s (hydrophone and vertical component) and 9.0 s (radial and transverse components) was used. The offset limit is especially desirable when either common conversion point (CCP) asymptotic binning or converted wave DMO is applied.

To obtain the correct geometry on Promax was very complicated and time consuming. Eventually, this problem was resolved using a land configuration. Some receivers had to have their positions corrected.

Two corrections were applied using true amplitude recovery: 1) geometrical spreading (spherical divergence) according to the inverse of the product of time and the square of velocity ($1/tv^2$, the velocity obtained from velocity analysis with a 1.5 km interval), and 2) 1.5 dB/sec correction. Correction for inelastic attenuation, with different values for the attenuation constant α was tested, but the results were not good and it was not applied.

Probably due to some acquisition gain problem, data from lines 33 to 37 have very low amplitudes. Surface consistent amplitude correction, using shot and receiver domains, solved this problem after three runs. Due to the presence of some extremely low frequency “bias” after the surface consistent amplitude was applied, a bandpass filter of 0-3-130-140 Hz was used.

Amplitude spectra show the presence of very strong notches in all components and at the hydrophone. These notches are likely caused by energy reverberation in the water layer, and will be discussed in more detail.

Velocity analysis was performed every 500 m, with the final velocities obtained after the second interpretation. In general, the velocity values are very low, as expected from the presence of gas. Sometimes, the definition of which velocity to be used was problematic, as two different hyperbolas cross each other. Because some events in the stacked sections correspond to reverberation, a minimum phase predictive decon (three gates, operator length and prediction distance varying) was applied after stacking.

From the three post-stack migration algorithms tested – phase-shift, finite difference and Kirchhoff – the last one was chosen. An AGC (1500 ms) was applied before migration, and the velocity used was 90% of the stacking velocity.

A bandpass time-varying filter and F-X Decon were applied after Kirchhoff migration in all sequences. The frequency ranges and time gates for the bandpass filter were obtained through spectral analysis using a 1.0 s window.

Hydrophone and Vertical Component

A conventional P-P analysis flow was applied on hydrophone and vertical component. A hydrophone gather, from a position out of the gas occurrence, is shown in Figure 2. Although many events are visible, probably some of them represent reverberations. On the amplitude spectrum of this gather (Figure 3), severe periodic notches, especially at around 10 and 20 Hz, are present. Between 30 and 100 Hz, the spectrum is approximately flat. Most of this energy is likely noise, as no such high frequency is expected. The steep descent above 110 Hz is due to the anti-alias filter applied during resampling.

A vertical component gather, also from out of the gas area, is shown on Figure 4. A cone of very low frequency and low velocity events (approximately between 130 and 250 m/s) at small offsets represents the Scholte wave – corresponding to the Stoneley wave in the land case. The spectrum of the data is shown in Figure 5. We note the anticipated exponential decrease of frequency.

The hydrophone and vertical component geophones migrated sections are presented in Figures 6 and 7, respectively.

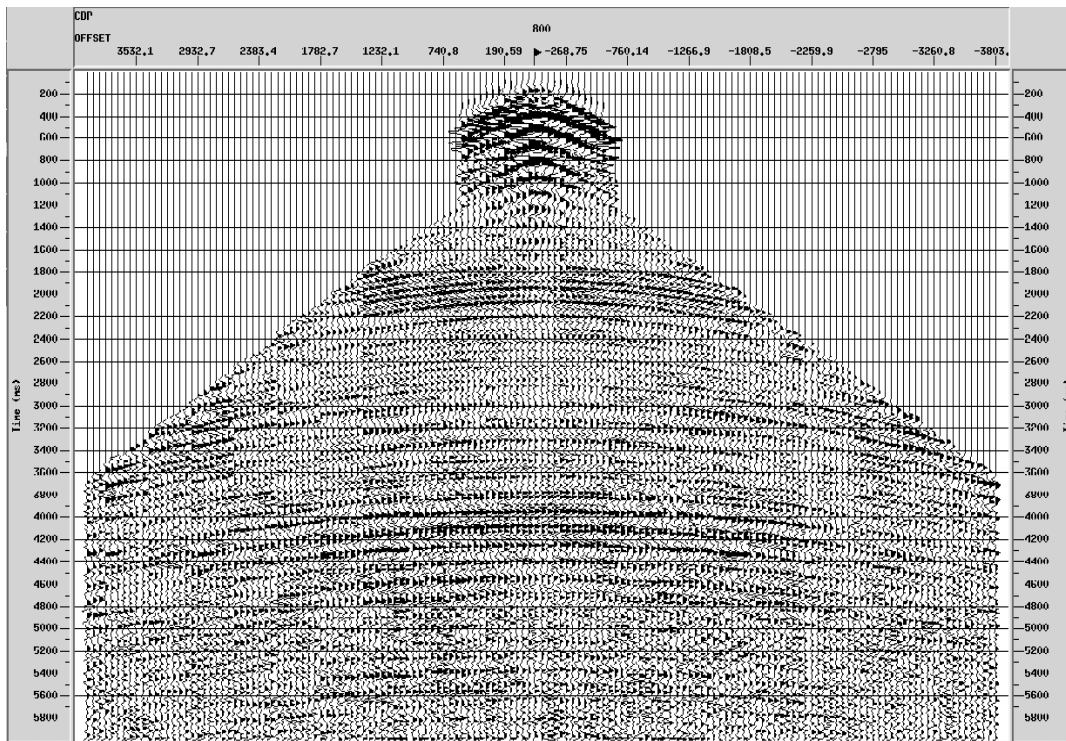


Fig.2. Hydrophone CDP gather (from a position out of the gas chimney)

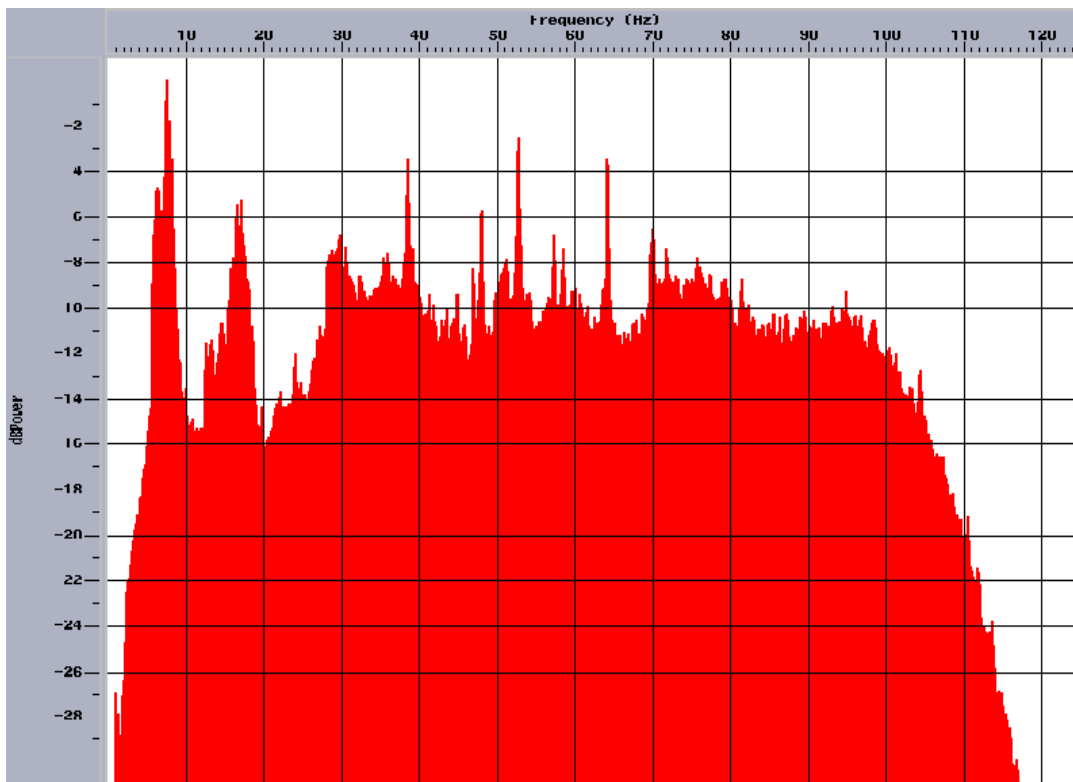


Fig. 3. Amplitude spectrum from hydrophone gather (fig. 2). Observe strong notches

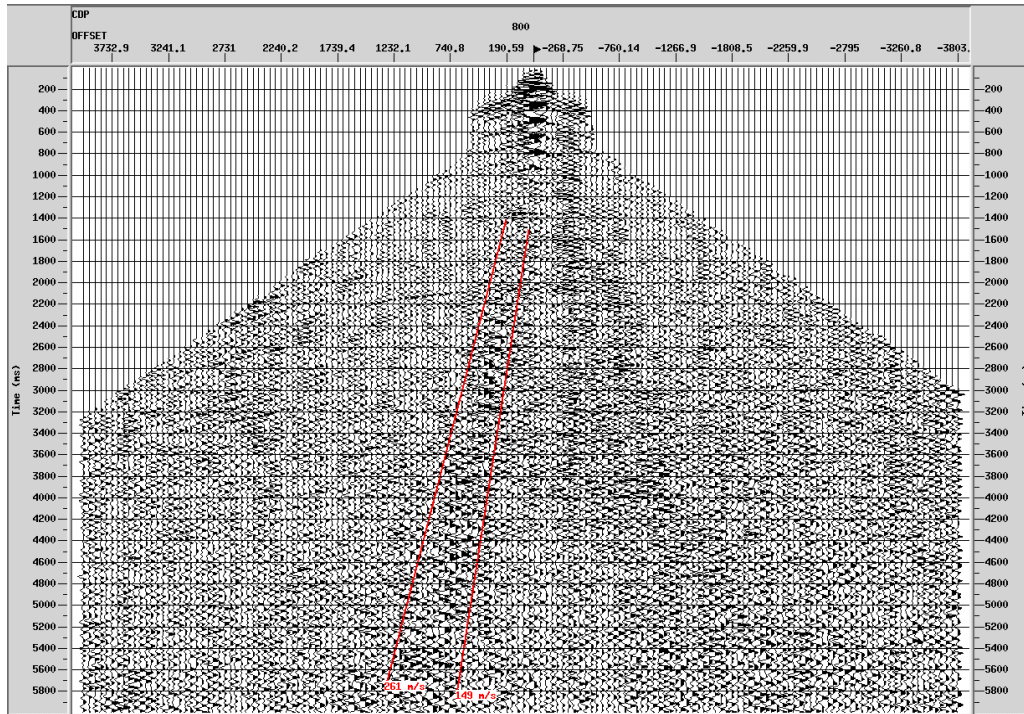


Fig. 4. Vertical component CDP gather (from a position out of gas chimney). Observe very low frequencies and velocities of Scholte waves.

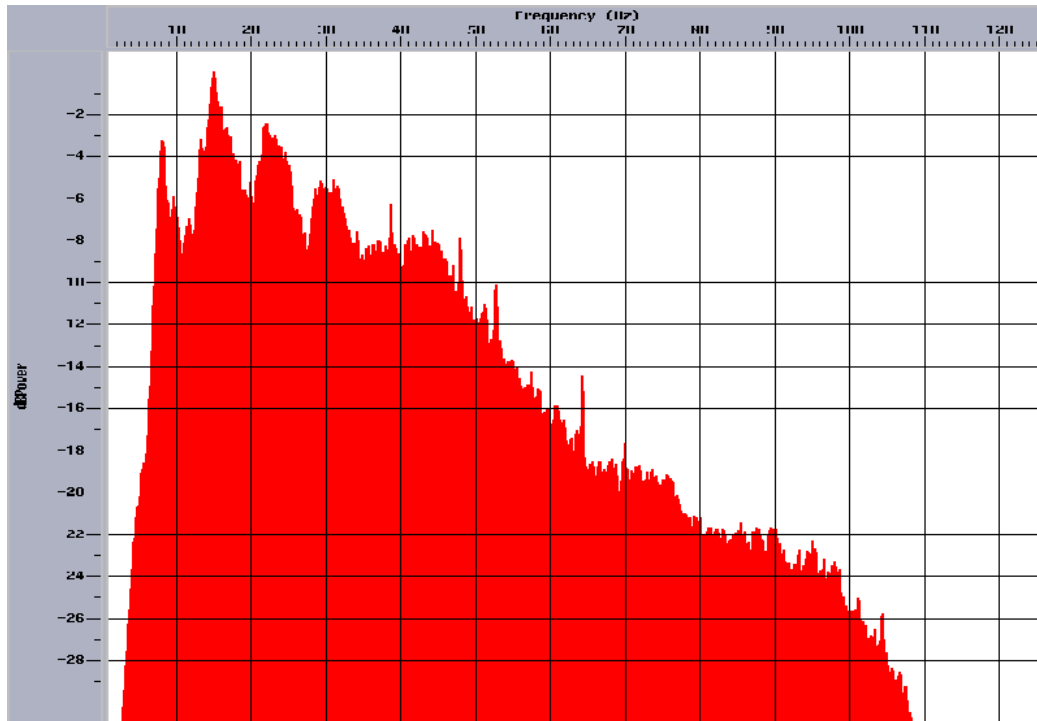


Fig.5. Amplitude spectrum from vertical component gather (fig. 4). Observe strong notches and energy decreases toward higher frequencies.

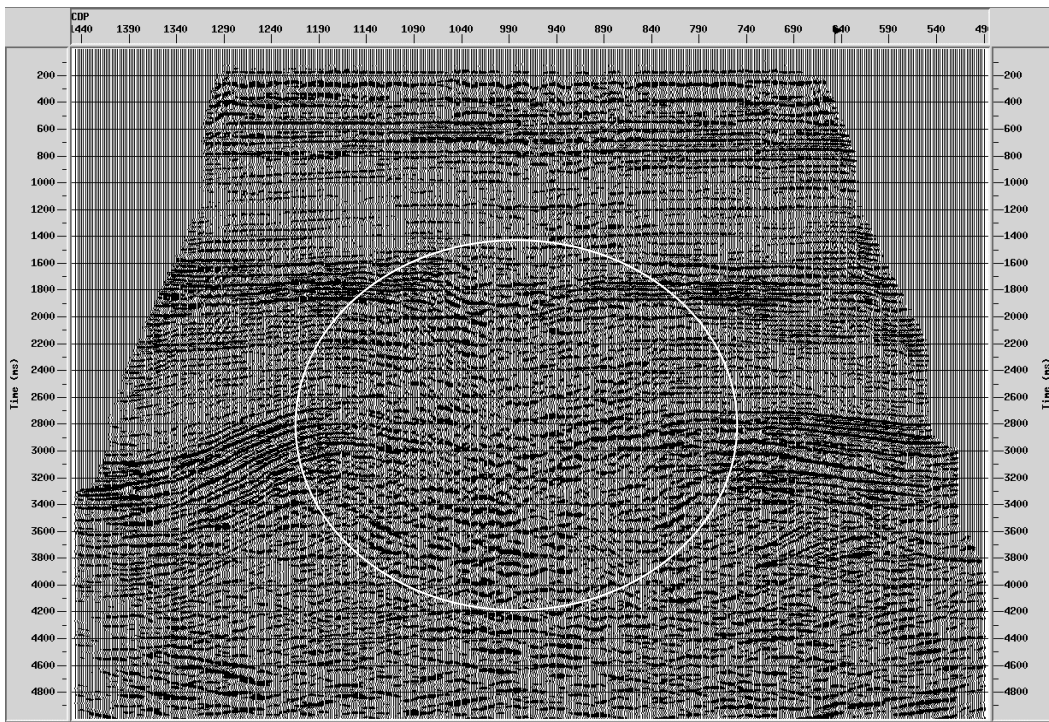


Fig. 6. Migrated section of hydrophone data. Observe pushdown and reflection-free zone at the center of the line.

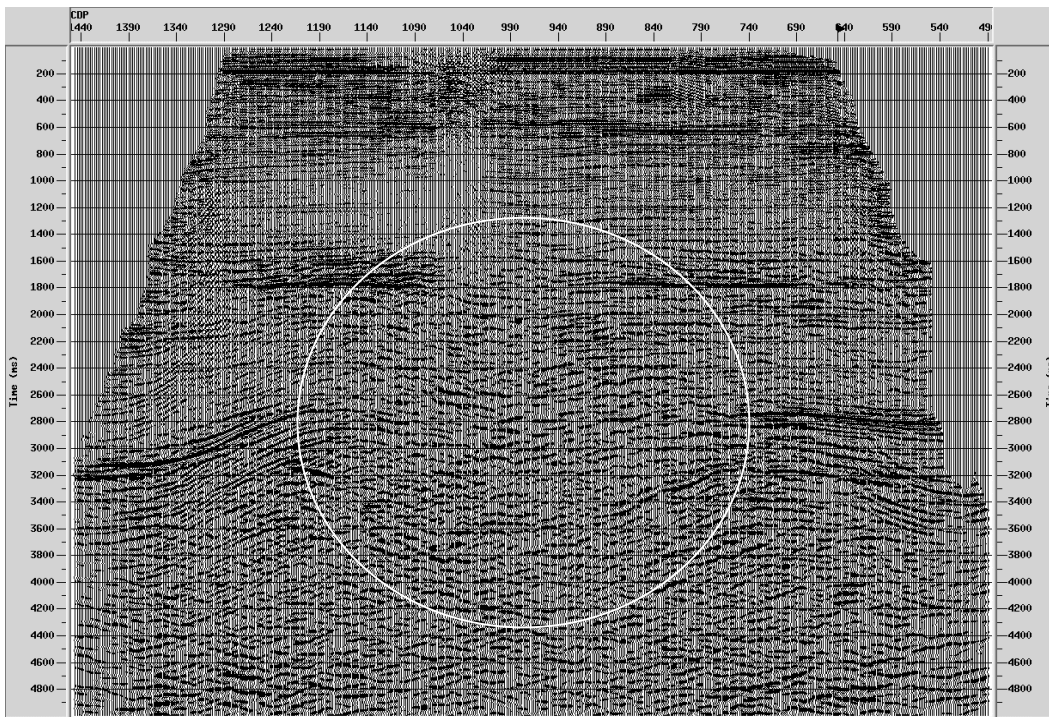


Fig.7. Migrated section of vertical component data.

Observations in published data from Valhall (D'Angelo et al., 1997, Leonard and Munns, 1987) permits us to conclude that the strong reflection from CDP 850 to north-east at 2.7 s, and its continuation to south-west after CDP 1150, is related to the top of the chalk (Paleocene Age), relative to both reservoir and pelagic facies. Another important event, between 3.1 s and 3.2 s on northeast of CDP 800, probably represents a Cretaceous unconformity. A pushdown effect is observed in the central part of the section, starting at 1.5s.

We interpret the reflection-free zone between CDPs 850 and 1100 below 2.3 s as being caused by the strong attenuation and scattering affecting P-wave propagation. This phenomenon is also present in other North Sea oil fields (e.g., Ekofisk). An almost horizontal and highly continuous event at 0.6 s is probably Miocene in age.

Radial Component

The processing sequence used here is based mainly on Harrison's (1992) work. The first step after resampling and geometry – which is the same for all components – was to perform a polarity reversal according to the relative position between source and receiver. Initially, a CDP processing flow was used to investigate whether P-S-S energy (shear-wave energy converted at the sea bottom) is present on the radial channel. Some reflections could be identified around 8.0 s (according to Thomsen et al., 1997, P-S-S reflections from target should occur at this time) when the lowest velocities present in semblance gathers were picked for stacking, but no continuity was present. More detailed processing – the equivalent offset migration (EOM) – is being evaluated now for P-S-S imaging.

Three different additional sequences were applied on the radial component: P-S asymptotic binning, converted-wave DMO, and equivalent offset migration.

Asymptotic binning finds the Common Conversion Point (CCP) using an asymptotic approximation algorithm (Tessmer and Behle, 1988) based on a V_p/V_s ratio. Initially, a constant value of 1.7 for the V_p/V_s ratio was used in the whole section. Landro et al. (1995) used an average V_p/V_s value of 1.4 for AVO analysis in the sediments from the water bottom to the target. A second processing run was performed with a ratio of 2.5, and much better results were obtained.

The asymptotic binning method assumes a small (<1.0) offset-to-depth ratio. For this reason, we compared stacked sections processed with 2.5 km offsets (close to the target depth, 2.4 km) and 4.0 km offsets to verify any possible problem in using the asymptotic approximation. We achieved better results for 4.0 km offsets, and this value was used during the processing.

A CCP gather, after asymptotic binning and NMO correction, is presented in Figure 8. We interpret the reservoir events between 5.0 and 5.5 s and the one immediately below 5.5 s. The high amplitude-low frequency reflections between 5.5 and 6.0 s may be due to reverberation from energy trapped inside the chalk layer (channel wave). This hypothesis follows from the high interval velocity observed in this layer, during velocity analyses.

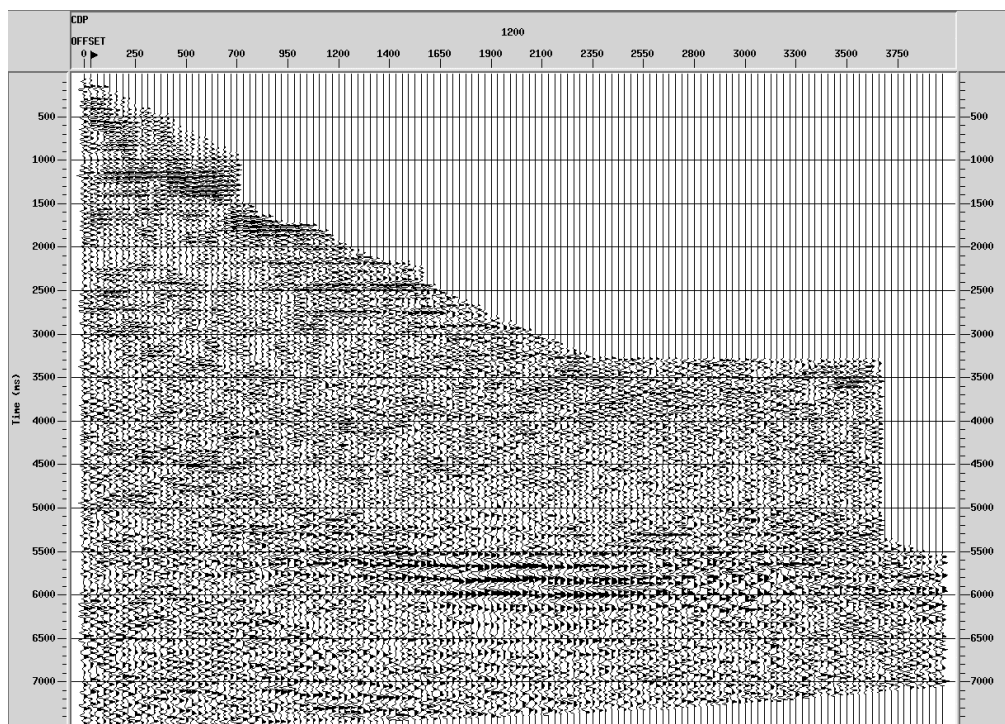


Fig.8. NMO-corrected common conversion point (CCP) gather of radial component data after asymptotic binning.

Figure 9 shows the spectrum for this CCP gather (without NMO correction). Clearly, the notches are present, although not at exactly the same frequencies as in the vertical component. These notches are problematic, as they are very strong over the frequency range where most of the converted wave energy usually occurs (8-25 Hz). We do need an algorithm to attenuate these effects, as is commonly done for the vertical component case (e.g., Barr and Sanders, 1989), using hydrophone information. Currently, a theoretical approach is being developed.

A pre-stack migration algorithm (Li and Bancroft, 1997) has been used to process this data. This migration method creates an intermediate pre-stack data volume, instead of directly obtaining the image section. This data volume is sorted into common scatter point (CSP) gathers, which provide migration velocity information.

One CSP gather at the same position as that of the CCP gather, from Figure 8, is presented in Figure 10. We can see similar events in the two gathers.

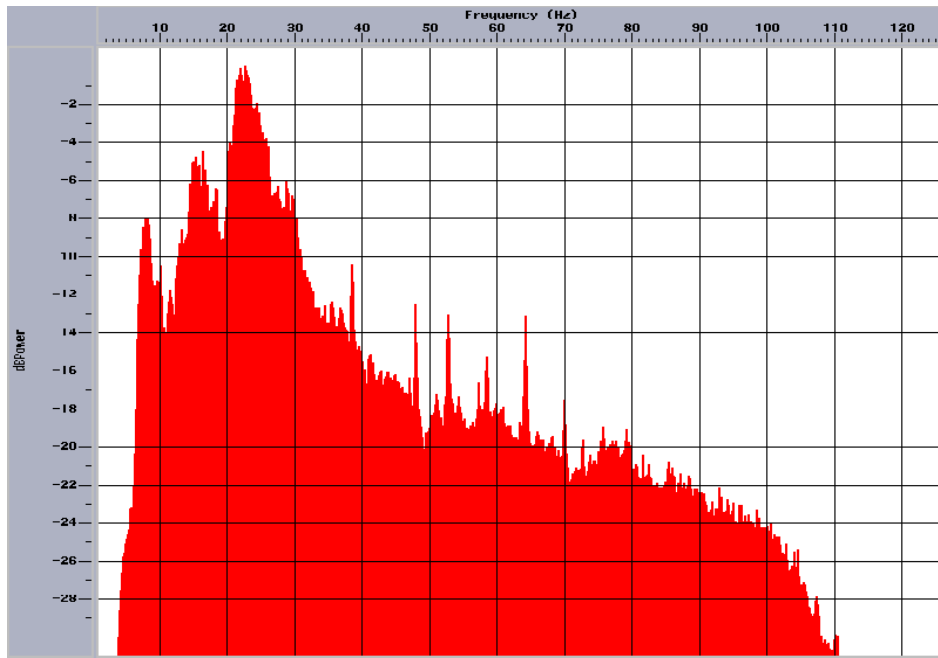


Fig.9. Amplitude spectrum of radial component CCP gather (fig. 8). Observe strong notches at signal bandwidth.

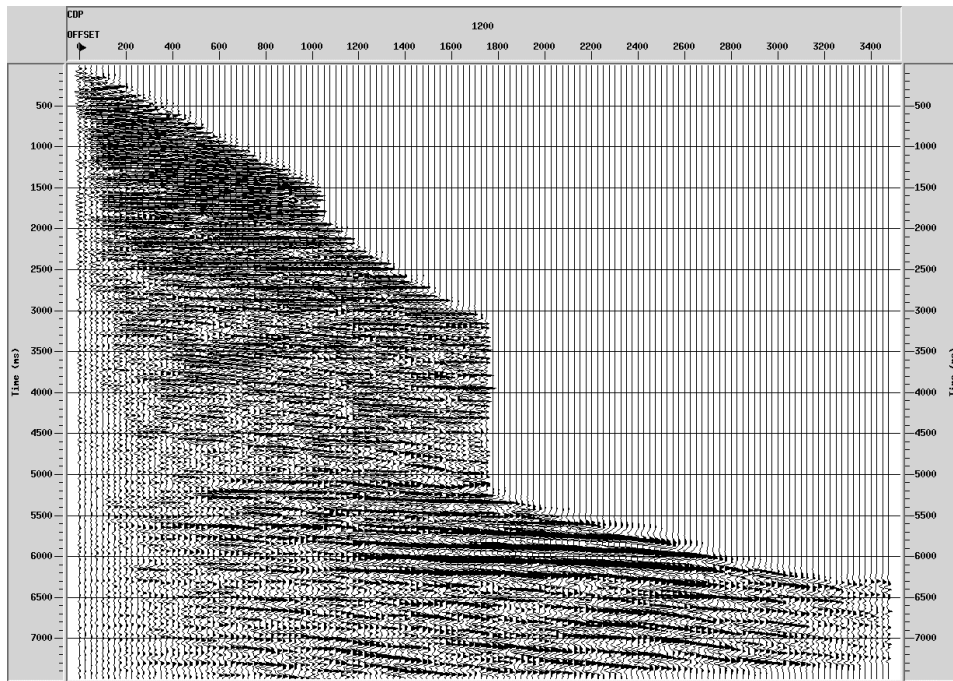


Fig. 10. NMO-corrected common scatter point (CSP) radial-component gather after equivalent offset migration (EOM). Observe higher energy content than CCP gather (fig. 8).

NMO correction with the migration velocity and conventional CDP stacking applied on CSP gathers complete the entire migration process. For the data presented here, the CPU time for this algorithm is close to the converted-wave DMO scheme.

A comparison of the amplitude spectra from the CSP (Figure 11) and CCP (Figure 9) gathers also shows some difference: neglecting the notch effect (which occurs approximately at the same frequencies in both cases), the CSP spectrum is somewhat flatter in the signal bandwidth (8-30 Hz). Two possible explanations are: 1) as the CSP method involves a collecting (stacking) of traces, it can act as a high-frequency filter, consequently increasing the relative energy in the lower frequency spectrum (Gary Margrave, personal communication), and/or 2) a Fresnel zone effect (Larry Lines, personal communication).

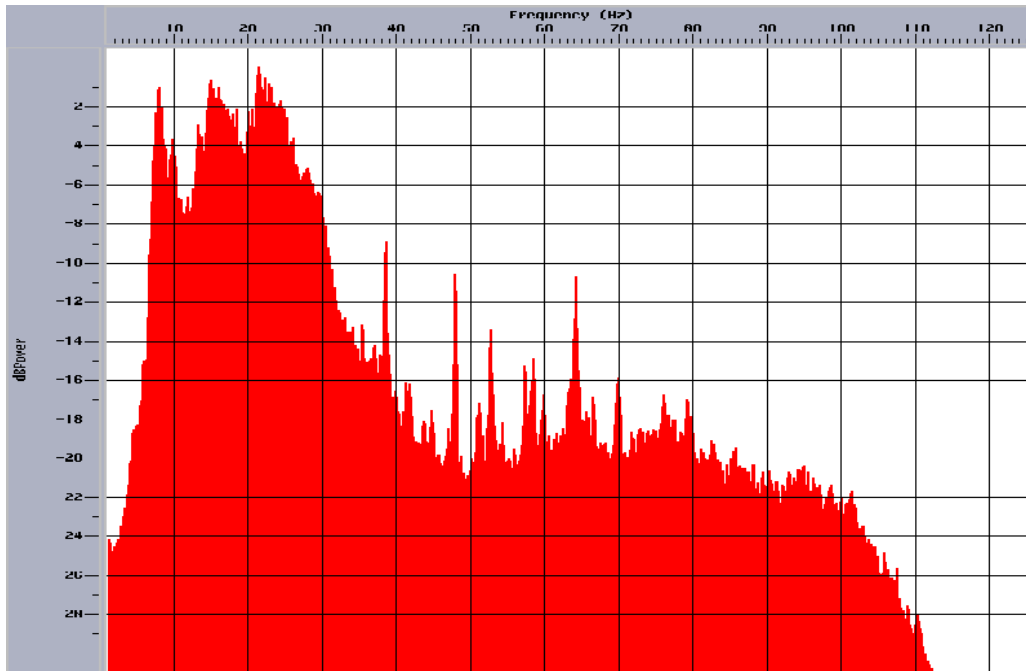


Fig.11. Amplitude spectrum of radial-component CSP gather (fig.10). Observe spectrum close to flat (neglecting notches) in the signal bandwidth.

In all three sequences (asymptotic binning, converted-wave DMO and EOM), the velocity interpretation was sometimes difficult due to lateral event discontinuity.

The CCP gather data were stacked with a V_p/V_s value of 2.5 – the result is shown on Figure 12. A quite continuous reflection, with relative high frequency, can be followed between 5.0 and 5.5 s in most of the line, and it probably is related to the top of the chalk. Some normal faulting seems to be present (e.g., CDPs 880 and 950). This is consistent with the tectonic evolution of this area (Leonard and Munns, 1987, D'Angelo et al., 1997). The result of the Kirchhoff migration is presented in Figure 13.

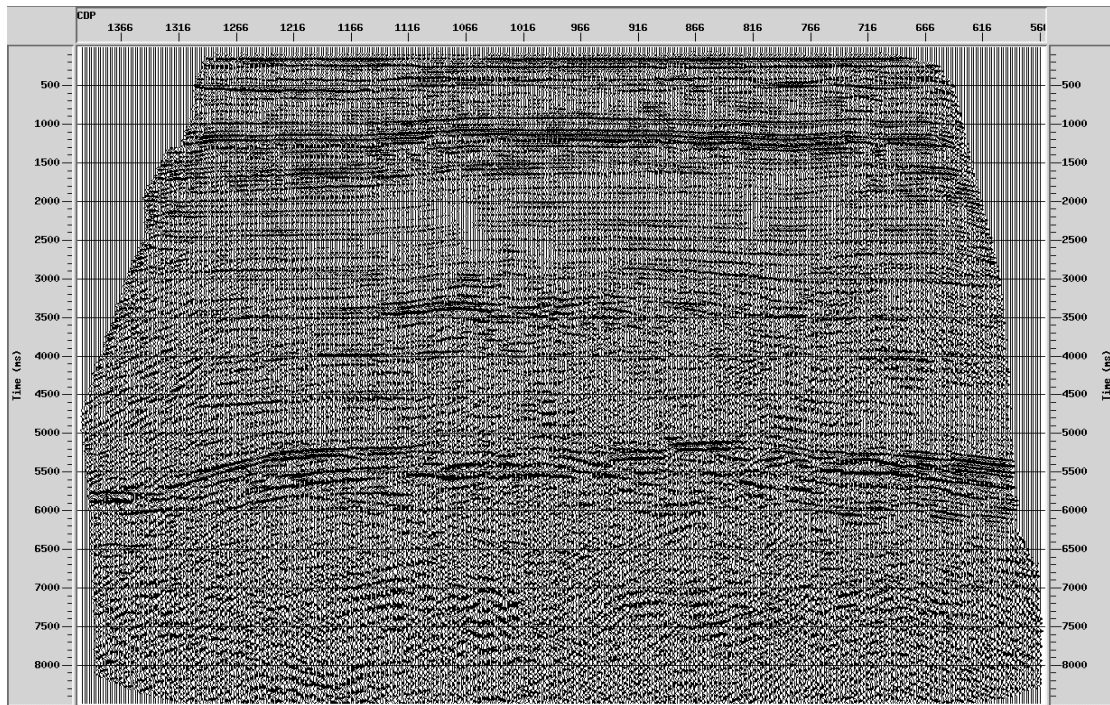


Fig. 12. Converted-wave stack ($V_p/V_s=2.5$) of CCP (asymptotic binning) radial-component data.

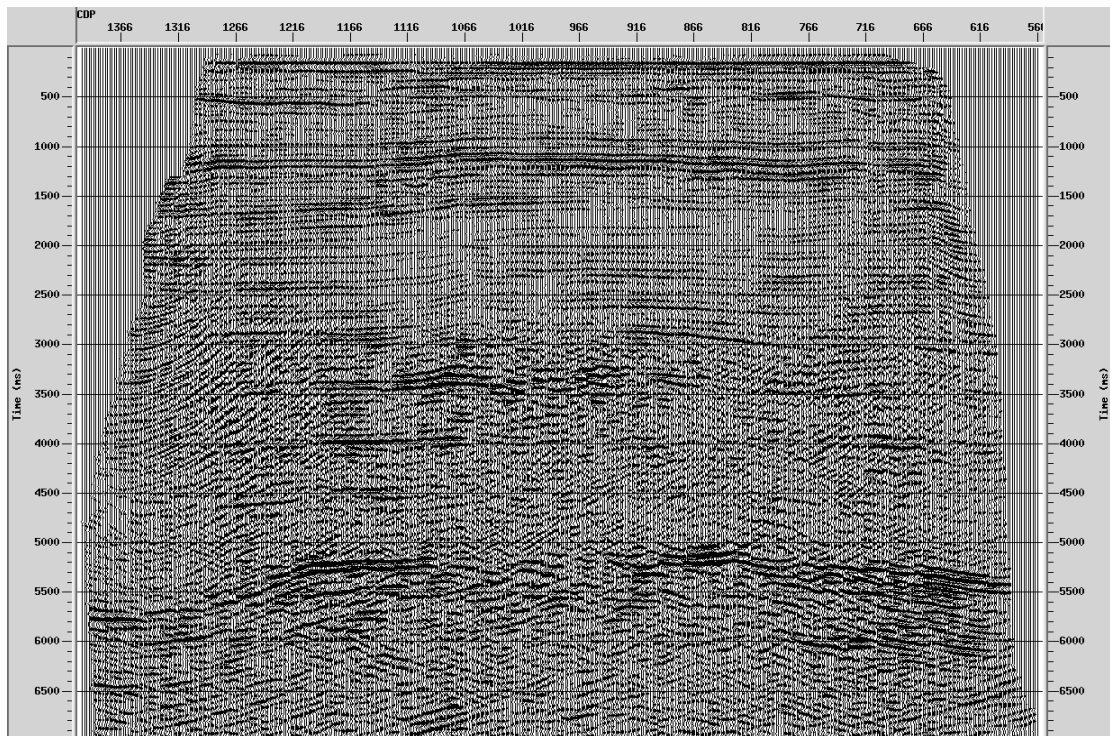


Fig.13. Kirchhoff migration on data from fig. 12.

The quality for this line is good, even if its central part has somewhat less continuity than on the structure's flanks. This may be due to the P-wave downgoing path inside the gas rich region and/or some fault imaging problem.

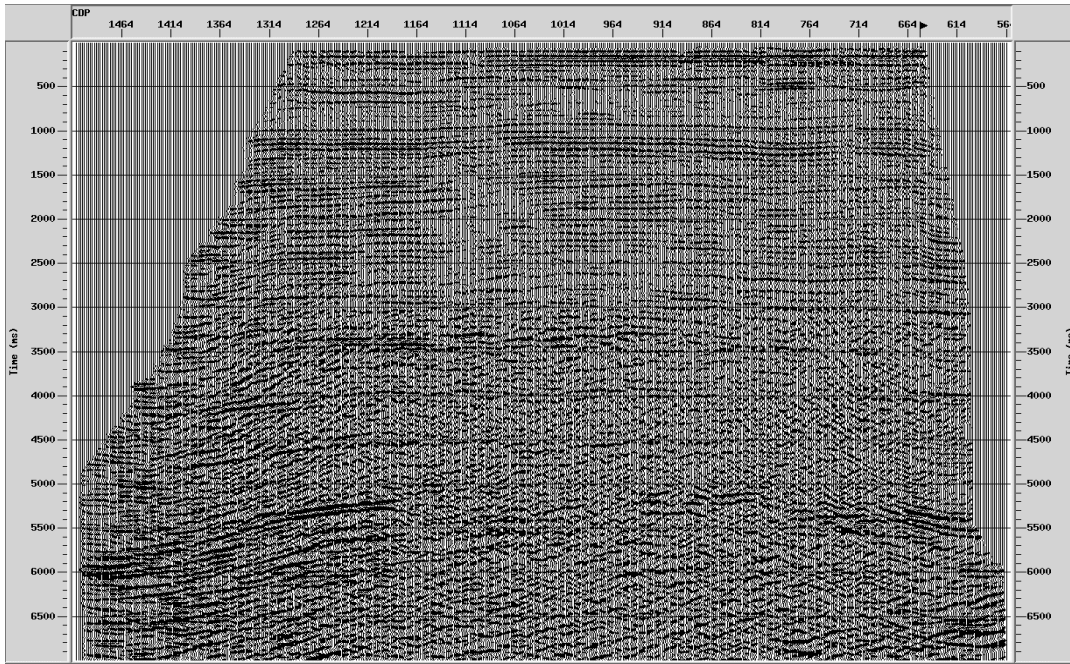


Fig.14. Converted-wave DMO, conventional stack, Kirchhoff migration on radial-component data. Compare with figures 13 and 15 (see text for discussion).

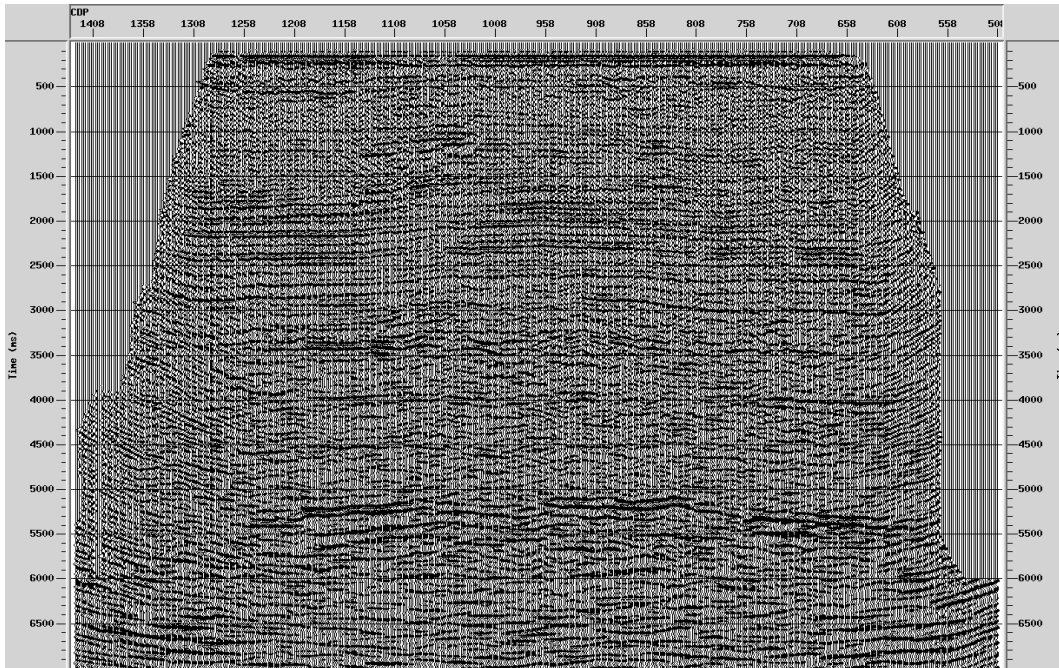


Fig.15. Equivalent-offset migration (EOM, or CSP binning) and conventional stack on radial-component data. Compare with figures 13 and 14 (see text for discussion).

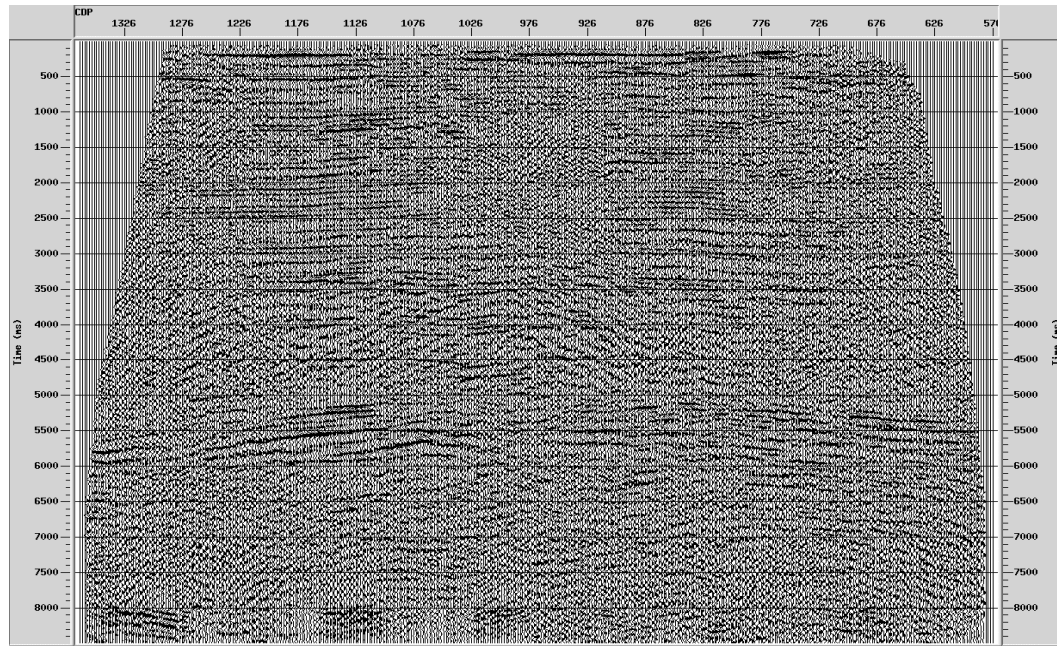


Fig.16. Converted-wave stack ($V_p/V_s=2.5$) of CCP (asymptotic binning) on transverse-component data.

Figure 14 shows the result from the sequence converted-wave DMO (no asymptotic binning applied), conventional stack and Kirchhoff migration on the radial data. A good image is obtained for the target at some parts of the line.

The final result for the EOM (CSP binning) method is shown in Figure 15. This process gives perhaps a better image than converted-wave DMO for the target. In this region (over the gas chimney), it also works a little better than the asymptotic binning. The EOM method, tested here for the first time on real P-S data, looks very promising in providing an image in an area with significant geophysical problems.

Transverse component

The asymptotic binning sequence applied in the radial component was used here. On CCP gathers not much energy seemed to be present. The stacked section (Figure 16) shows some coherent events. This energy may be associated with acquisition misalignments, lateral reflections, or anisotropy.

P-S flow in vertical component, P-P flow in radial and transverse components

A test was performed to investigate both the presence of S-wave energy on the vertical component and P-wave energy on the radial and transverse components. We applied the vertical component processing flow (and velocities) in radial and transverse components and the asymptotic binning flow (with corresponding velocities) on the vertical channel. The resulting stacked sections for vertical (Figure 17) and radial (Figure 18) components indicate that there is not very much cross-coupled energy.

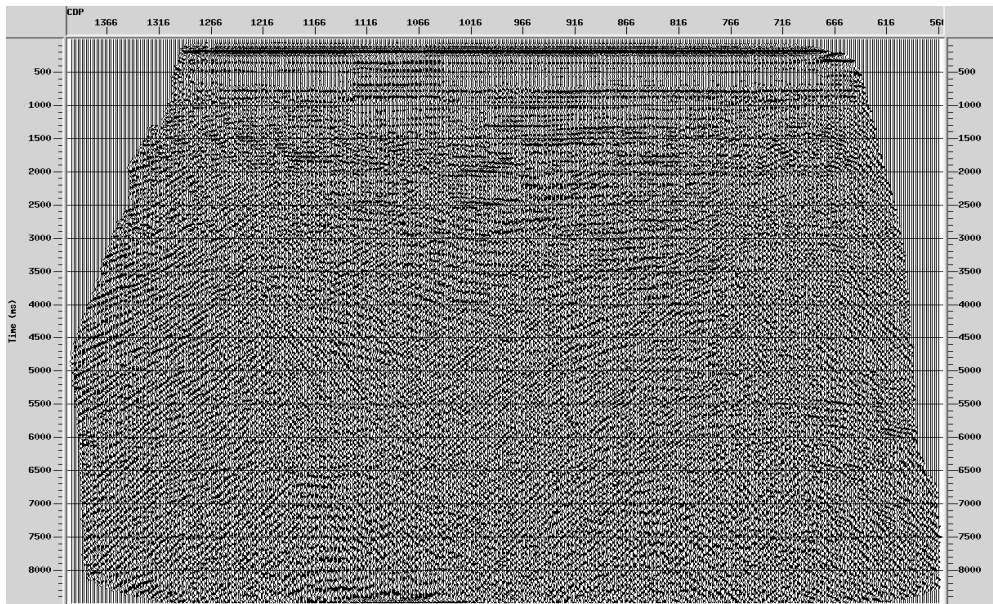


Fig.17. P-S flow (asymptotic binning and converted-wave stack) applied in vertical-component data.

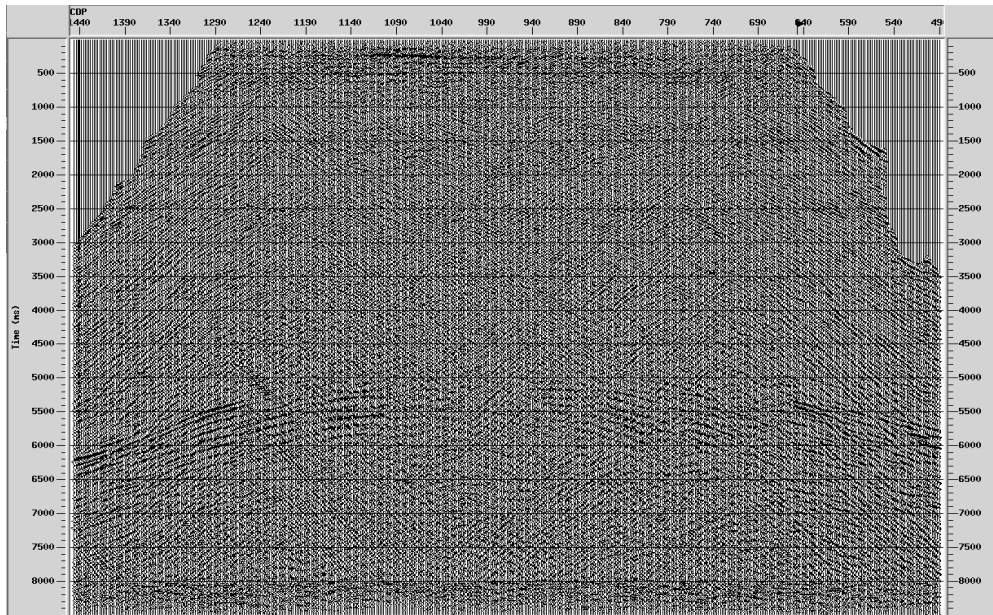


Fig.18. P-P flow applied in radial-component data.

CONCLUSIONS

The hydrophone and vertical component do not provide interpretable images of the reservoir region. The radial component gives reasonable P-S images. A comparison among three methods for P-S processing (CCP asymptotic binning, converted-wave DMO and EOM) showed that all methods provided some areas of preferred quality. The EOM method shows considerable promise. Some energy is present in transverse component, and there are various explanations possible. Very

little shear energy is present on the vertical component, and the same is true for compressional energy on radial and transverse data. Strong notches are present in all geophone components and in the hydrophone; these notches are especially problematic on the radial data, as they occur at the signal bandwidth. Geophone coupling and receiver positioning seem not to be a problem for this survey.

ACKNOWLEDGMENTS

We are grateful to Amoco Exploration and Production, Amoco Norway and their partners in the Valhall License (Amerada Hess Norge, Elf Petroleum Norge and Enterprise Oil Norge) and PGS Norway for the permission to present this data. Many thanks to Christian Strand, from PGS Norway, and Mark Harrison, from Matrix Geoservice Ltd., for all the information about the acquisition and discussions on processing. We also appreciate the comments of Prof. Gary Margrave and Prof. Larry Lines. To CREWES staff and students, for their support with Promax, and to Ms. Medina Deuling (Department of Geography), for the coordinate conversion.

REFERENCES

- Barr, F.J. and Sanders, J.I., 1989, Attenuation of water-column reverberations using pressure and velocity detectors in a water-bottom cable: Presented at the 59th Annual SEG Meeting.
- Berteussen, K.A., Fromyr, E., Rokkan, A., Langhammer, J. and Strand, C., 1997, Acquisition of multi component data by 'Dragged Array': Presented at the 59th EAGE Conference & Tech. Exhibition.
- D'Angelo, R.M., Brandal, M.K. and Rorvik, K.O., 1997, Porosity detection and mapping in a basinal carbonate setting, Offshore Norway, in Carbonate Seismology, edited by Ibrahim Palaz and Kurt J. Mafurt, Geophysical Developments Series, # 6, SEG.
- Farmer, C.L. and Barkved, O.I., 1997, Influence of syn-depositional faulting on thickness variations in chalk reservoirs – Valhall and Hod Fields. Petroleum Geology of Northwest Europe: Proceedings of the 5th Conference. Geological Society of London.
- Harrison, M.P., 1992, Processing of P-SV Surface-Seismic Data: Anisotropy Analysis, Dip Moveout, and Migration. Ph.D. Thesis, The University of Calgary.
- Kommedal, J.H., Barkved, O.I. and Thomsen, L.A., 1997, Acquisition of 4 Component OBS Data – a case study from the Valhall field: Presented at the 59th EAGE Conference & Tech. Exhibition.
- Landro, M., Buland, A. and D'Angelo, R., 1995, Target-oriented AVO inversion of data from Valhall and Hod fields: *The Leading Edge*, 14(8): 855-861.
- Leonard, R.C. and Munns, J.W., 1987, Valhall, in *Geology of the Norwegian Oil and Gas Fields*, edited by A.M. Spencer *et al.* Graham & Trotman, 493 p.
- Li, X. and Bancroft, J.B., 1997, Converted wave migration and common conversion point binning by equivalent offset: Presented at the 67th Annual SEG Meeting.
- Munns, J.W. and Mullen, D., 1987, Fault Detection using Borehole Seismic Surveys, in *Atlas of Seismic Stratigraphy*, AAPG Studies in Geology # 27, vol. 1, p. 117-118.
- Tessmer, G. and Behle, A., 1988, Common Reflection Point Data-Stacking Technique for Converted Waves: *Geophysical Prospecting*, 36:671-688.

Thomsen, L.A., Barkved, O.I., Haggard, B., Kommedal, J.H. and Rosland, B., 1997, Converted-wave Imaging of Valhall Reservoir: Presented at the 59th EAGE Conference & Tech. Exhibition.